Tumor regrowth between surgery and initiation of adjuvant therapy in patients with newly diagnosed glioblastoma

Andrea Pirzkall, Colleen McGue, Suja Saraswathy, Soonmee Cha, Raymond Liu, Scott Vandenberg, Kathleen R. Lamborn, Mitchel S. Berger, Susan M. Chang, and Sarah J. Nelson

Department of Radiology and Margaret Hart Surbeck Laboratory of Advanced Imaging (A.P., C.M., S.S., S.C., S.J.N.), Department of Neurological Surgery (A.P., S.C., R.L., S.V., K.R.L., M.S.B., S.M.C.), and Department of Radiation Oncology (A.P.), University of California, San Francisco, San Francisco, CA, USA

To assess incidence and degree of regrowth in glioblastoma between surgery and radiation therapy (RT) and to correlate regrowth with presurgical imaging and survival, we examined images of 32 patients with newly diagnosed glioblastoma who underwent MR spectroscopic imaging (MRSI), perfusion-weighted imaging (PWI), and diffusion-weighted imaging (DWI) prior to surgery, after surgery, and prior to RT/temozolomide. Contrast enhancement (CE) in the pre-RT MR image was compared with postsurgical DWI to differentiate tumor growth from postsurgical infarct. MRSI and PWI parameters were analyzed prior to surgery and pre-RT. Postsurgical MRI indicated that 18 patients had gross total and 14 subtotal resections. Twenty-one patients showed reduced diffusion, and 25 patients showed new or increased CE. In eight patients (25%), the new CE was confined to areas of postsurgical reduced diffusion. In the other 17 patients (53%), new CE was found to be indicative of tumor growth or a combination of tumor growth and surgical injury. Higher perfusion and creatine within nonenhancing tumor in the presurgery MR were associated with subsequent tumor growth. High levels of choline and reduced diffusion in pre-RT CE suggested active metabolism and tumor cell proliferation. Median survival was 14.6 months in patients with interim tumor growth and 24 months in patients with no growth. Increased volume or new onset of CE between surgery and RT was attributed to tumor growth in 53% of patients and was associated with shorter survival. This suggests that reducing the time between surgery and adjuvant therapy may be important. The acquisition of metabolic and physiologic imaging data prior to adjuvant therapy may also be valuable in assessing regions of new CE and nonenhancing tumor. *Neuro-Oncology 11, 842–852, 2009 (Posted to Neuro-Oncology [serial online], Doc. D08-00064, February 19, 2009. URL http://neuro-oncology.dukejournals.org; DOI: 10.1215/15228517-2009-005)*

Keywords: brain glioma, extent of resection, GBM, glioblastoma, MRI, tumor growth

Glioblastoma is the most malignant brain tumor in adults. It is heterogeneous in appearance and outcome. The survival for most patients remains dismal despite aggressive multimodal therapeutic strategies. The standard of care for patients with a newly diagnosed glioblastoma entails surgical resection and concurrent radiation therapy (RT) and chemotherapy. Chemotherapy includes temozolomide and is typically continued for 6 months or until tumor progression. The resulting median survival is 15 months.[1] Few patients survive long term—the 5-year survival rate is less than 2%.[2] Methods for predicting individual patient outcome

Received March 12, 2008; accepted September 23, 2008.

Address correspondence to Andrea Pirzkall,Genentech, Inc., 1 DNA Way, Mail Stop 442a, South San Francisco, CA 94080, USA (pirzkall.andrea@gene.com).

are highly sought after in order to improve patient management and selection for suitable and/or experimental treatment protocols. Clinical factors that have been reported to be associated with a more favorable prognosis include age less than 45 years and better preoperative KPS score.[3–5] The extent of resection has been suggested as a prognostic factor in glioblastoma but remains controversial.[4,6,7] Molecular markers that have been reported as having prognostic significance include Ki-67[8,9] and O^6-methylguanine-DNA methyltransferase (*MGMT*) promoter status.[10]

The assessment of the extent of surgical resection is based on an immediate postoperative MRI, which needs to be acquired within the first 3 days (preferably within the first 24 h) after surgery to avoid the confounding effects of surgically induced contrast enhancement (CE).[6,11–13] Recent studies have shown that when diffusion-weighted imaging (DWI) is performed as part of the routine postoperative MRI, it is able to prevent misinterpretation of CE on subsequent scans. Diffusion-weighted abnormalities (DWA) adjacent to or along the resection cavity and that were not attributable to blood products (no intrinsic shortening on T1-weighted MR images) became enhancing in 64%–70% of patients with newly diagnosed glioblastoma.[14,15] These regions were interpreted as postoperative ischemia and ultimately turned into regions with cystic encephalomalacia that were seen on T2-weighted MR images between 55 and 200 days postsurgery. The CE pattern in spatial correspondence with this effect occurred within 15–75 days postsurgery and was most likely related to postoperative infarct that would otherwise be mistaken as tumor progression.

Adjuvant therapy consisting of concurrent RT and chemotherapy is usually not initiated until 4–5 weeks postsurgery in order to allow sufficient recovery time and to permit wound healing. It has not been shown whether a delay in initiation of such adjuvant therapy affects tumor regrowth and outcome. MR images are not routinely acquired immediately prior to RT, and treatment planning is typically carried out based on CT in correlation with the immediate postsurgical MRI. Determining whether there are differences between MR images acquired at the postsurgical exam and those acquired prior to RT is important for patient management.

The major objective of this study was to assess the incidence and degree of tumor regrowth in patients with newly diagnosed glioblastoma between surgical resection and initiation of RT. A second objective was to see whether tumor regrowth correlated with MIB-1 labeling as a surrogate marker of proliferative capacity. A third objective was to determine whether imaging parameters that were obtained at initial diagnosis and prior to surgery would be predictive of aggressive tumor behavior. To evaluate the significance of such data, we then compared quantitative imaging parameters acquired at both time points for patients with and without interim tumor regrowth and correlated the results with survival.

Materials and Methods

Thirty-two patients with newly diagnosed glioblastoma underwent advanced MRI at multiple time points: prior to surgery, immediately after surgery, prior to RT (pre-RT), upon concluding RT, and at 2 and 4 months thereafter. All MR studies included anatomic MRI, DWI, perfusion-weighted imaging (PWI), and MR spectroscopy imaging (MRSI), with the exception of the immediate postsurgical imaging, which consisted only of anatomic MRI and DWI. Diagnosis of a glioblastoma was made in accordance with the WHO classification[16] upon histopathologic and immunohistochemical analysis of tissue following maximal safe surgical resection. MIB-1 labeling index was determined in all tumors. *MGMT* promoter methylation status was not available in all tumors and is not controlled for in this study.

Adjuvant therapy was initiated a median of 32.5 days (range, 14–46 days) following surgery and consisted of concurrent RT and chemotherapy. RT was carried out following three-dimensional conformal treatment planning with standard target definition based on treatment planning CT in conjunction with pre-RT anatomic MRI, administering a total dose of 60 Gy over a course of 6 weeks (standard fractionation of 2 Gy/day). Chemotherapy was given concurrently either as temozolomide alone (13 patients), temozolomide in combination with Tarceva (9 patients), poly-ICLC (4 patients), R115777 (a farnesyl transferase inhibitor; 1 patient), Accutane and Celebrex (1 patient), tamoxifen and thalidomide (1 patient), bischloroethyl nitrosourea (carmustine) and tamoxifen (1 patient), and antineoplastons (1 patient). One patient did not receive adjuvant chemotherapy.

Imaging Modalities and Acquisition Parameters

All presurgical and postsurgical imaging studies were acquired on a 1.5-T GE Signa Echospeed MR scanner (GE Medical Systems, Milwaukee, WI, USA). Pre-RT and subsequent imaging studies were acquired on either a 1.5-T or a 3-T GE Signa Echospeed MR scanner using commercially available head coils. All patients provided informed consent for participating in the study based on a protocol approved by the University of California, San Francisco Committee on Human Research.

Anatomic MRI. The MRI protocol consisted of T1-weighted (repetition time [TR]/echo time [TE] = 400/12 ms) sagittal scout images; axial FLAIR (fluid-attenuated inversion recovery) images [TR/TE/T1 = 1,000/143/2,200 ms, $220 \times 220 \times 160$ mm^3 field of view (FOV) with $256 \times 256 \times 32$ matrix]; and pre- and post-contrast T1-weighted volume SPGR (spoiled gradient echo) images (TR/TE = 32/8, 40 flip angle, $180 \times 240 \times 186$ mm^3 FOV with $192 \times 256 \times 124$ matrix). The FLAIR and pregadolinium SPGR images were aligned with the postgadolinium SPGR images using software developed in our laboratory.[17]

Perfusion-Weighted Imaging. A gadolinium diethyl enetriamine-pentacid (Gd-DTPA) bolus of 0.1 mmol/kg body weight was injected rapidly into the antecubital vein using an automatic injector (Medrad, Pittsburgh, PA, USA) at a rate of 5 ml/s. Dynamic susceptibility contrast echo planar (EPI) gradient echo (GE) images were acquired before, during, and after the bolus injection. PWI parameters were TR/TE 1,500/54 ms, 35° flip angle, 26 × 26 cm^2 FOV, 128 × 128 acquisition matrix, 4-mm slice thickness, and a total of 80 time points. Perfusion data sets were processed to yield the height of the peak in the concentration time curve during delivery of the bolus (ΔR2* peak height [PH]) and percent ΔR2* recovery to baseline levels, as well as the area under the curve (relative cerebral blood volume [CBV]), using in-house software.[18] Perfusion-derived maps were calculated and normalized to the peak of a model curve function derived from normal-appearing brain, resampled to the same resolution as the SPGR images, and rigidly aligned to the SPGR using the open-source Visualization Toolkit (VTK) software package (http://www.vtk.org).

Diffusion Tensor Imaging. An EPI spin echo diffusion tensor pulse sequence was used to acquire images that covered the supratentorial brain. Diffusion tensor imaging (DTI) parameters were TR/TE = 10,000/100 ms, matrix 128 × 128 × 28, FOV = 360 × 360 mm^3, 3-mm slice thickness, b value = 1,000 s/mm^2, gradient strength = 0.04 T/m, gradient duration = 21 ms, and gradient separation = 27 ms. The apparent diffusion coefficient (ADC) and fractional anisotropy maps were calculated by the pixel-by-pixel–based MR signal intensity decay from DTI using software developed in-house. Diffusion maps were normalized relative to the mean of the voxels in normal-appearing white matter, resampled to the same resolution as the SPGR images, and rigidly aligned to them using VTK software.

Proton (^{1}H) MRSI. Three-dimensional MRSI (TR/TE = 1,000/144 ms, phase encoding matrix = 12 × 12 × 8 or 16 × 8 × 8) with 1-cc nominal resolution was acquired with point-resolved spectroscopic (PRESS) volume localization and very selective saturation bands[19] for outer voxel suppression using the axial FLAIR image as a reference. The PRESS box was positioned to cover both the lesion and 200–300 cc of normal-appearing tissue. Areas of subcutaneous lipids and varying magnetic susceptibility that might compromise the quality of the spectra were avoided. Among the patients who received spectroscopy prior to adjuvant therapy (pre-RT), 65% received lactate-edited spectroscopy as described previously.[20] The ^{1}H MRSI processing algorithms were developed in-house and have been applied to a large number of patients.[21,22] Briefly, the data were filtered with a Lorentzian function and Fourier transformed, resulting in an array of spectra. The spectra were corrected for baseline variations, phase shifts, and frequency shifts within the region of each peak, employing a priori information about the relative location of each metabolite peak. An automatic search procedure was used to identify each resonance. The peak height values for choline (Cho), creatine (Cr), *N*-acetylaspartate (NAA), combined lactate/lipid, or, in the case of lactate-edited acquisition, separate lactate and lipid resonances were quantified. Spectral values were normalized relative to the noise levels at the right-hand end of the spectra. A Cho-to-NAA index (CNI), which defines the distance between the Cho:NAA ratio for a given voxel and a regression line fit to the Cho:NAA ratio of the normal voxels in a given subject, was calculated for each voxel for all patients, using an automated technique described elsewhere.[23] Similarly, indices for Cho and Cr (CCrI) and for Cr and NAA were calculated. Quantified metabolic maps were resampled with sinc interpolation to the same resolution as the SPGR. The spectroscopic data were assumed to be in alignment with the postgadolinium SPGR images since the ^{1}H MRSI examination was acquired shortly afterward.

All imaging modalities were rigidly aligned and resampled to the resolution of the postcontrast SPGR data set of each respective imaging time point in order to allow for a region-of-interest (ROI) analysis of corresponding spatial location.

Imaging Analysis

Visual Assessment. Visual assessments were made by three independent readers: a neuroradiologist (S.C.), a neurooncologist (S.M.C.), and a radiation oncologist (A.P.). Disagreement occurred in 4 of 32 cases and was consolidated among all three readers thereafter.

Postsurgery imaging: Extent of resection and presence of postsurgical injury were assessed based on postsurgical MRI and DWI. Extent of resection was considered gross total (GTR) if no CE tumor components remained, and subtotal (STR) if CE residual tumor remained. Likelihood of postsurgical injury was visually assessed based on postsurgical DWI whereby hypointense regions with ADC values of less than 500 × 10^{-6} mm^2/s around or remote from the resection cavity were deemed abnormal (DWA).[14] A thin and linear rim of reduced diffusion around the resection cavity without focal nodularity was not considered abnormal.

Pre-RT imaging: Presence of new CE was assessed based on the pre-RT postcontrast SPGR (accounting for possible regions of intrinsic T1 shortening indicative of blood products as assessed on precontrast SPGR). Regions of new CE were visually compared to the extent of reduced diffusion seen on postsurgical DWI to differentiate tumor growth from postsurgical injury. Based on pre-RT MRI, patients without new CE or with new CE in spatial correspondence to regions of reduced diffusion on postsurgical DW images were categorized as having "no growth." In contrast, new CE at pre-RT that either was spatially unrelated to postsurgically reduced diffusion and therefore considered indicative of tumor growth, or that coincided with postsurgically reduced diffusion only in some portions, was considered a combination of surgical injury and tumor growth; those patients were categorized as having "tumor growth."

Quantitative Imaging. At pre-RT, regions of new CE were manually outlined (C.M.), verified (A.P.), and saved according to the classification of "tumor growth" or "no growth" as outlined above. Respective volumes and quantitative MRI parameters were calculated within the regions of new CE.

Prior to surgery, the CE and nonenhancing component of the tumor were defined based on postcontrast SPGR and FLAIR imaging, respectively, by means of semiautomated segmentation tools developed in-house. The presurgery ROIs were then visually verified for accuracy (C.M., A.P.). Quantitative MRI parameters were calculated within these mutually exclusive regions and compared between both patient groups in order to determine whether presurgical imaging parameters might be predictive of interim tumor growth and thereby indicative of more aggressive behavior.

Statistics

In order to compare presurgical and pre-RT imaging parameters and MIB-1 labeling index in patients with tumor growth versus no growth, a Wilcoxon-Mann-Whitney two-sample test was applied. Survival was estimated using Kaplan-Meier curves. Log-rank and two-tailed Wilcoxon tests were applied to test for a possible difference in survival between the two patient groups. The log-rank test is more sensitive to differences between groups at later time points, whereas the Wilcoxon test is more sensitive to test differences between groups that occurred in early time points.

Survival was calculated as the time from pre-RT imaging to date of death or date last known alive and censored accordingly. We chose the pre-RT imaging date as the reference for our survival analysis (as opposed to the standard date of surgery) because we sought to test the predictive value for survival for patients who showed tumor growth versus no growth as assessed on pre-RT imaging. In doing so, we eliminated a possible contribution of varying time intervals between surgery and pre-RT imaging.

All imaging variables described above were compared between both groups, correlated with MIB-1 labeling, and considered as predictors of outcome. Results are reported as a possible trend ($0.05 < p < 1.0$) or as significant ($p < 0.05$). p-Values are reported without adjustment for multiple comparisons. Because of the large number of comparisons, there is increased likelihood that some differences may be due to chance. The relatively small number of cases increases the likelihood that some true differences will not be identified as statistically significant due to limited power. Thus, the results of the statistical tests should be considered as an adjunct to the estimation with the intent to show the pattern observed in the data, and not as proof of a specific hypothesis. For example, the use of two different test procedures in assessing the survival differences provides information on the nature of the difference in survival observed.

Results

Patient characteristics for both patient groups with tumor growth versus no growth, including the extent of surgery, MIB-1 labeling, and survival, are summarized in Table 1. Presurgical imaging was acquired 1 day prior to surgery (range, 0–2 days). Pre-RT imaging was acquired 14–48 (median 27) days following surgery and 5–21 (median 6) days prior to RT. RT was initiated 14–46 (median 32.5) days after surgery.

Status Postsurgery

Extent of Resection. Eighteen patients (56%) were considered to have undergone GTR and 14 patients (44%) STR. For STR, estimated degree of enhancing tumor tissue that was removed ranged from 70% to 95% (median, 90%). The large amount of tissue removed and the high rate of GTR reflect the approach of maximal safe resection that is practiced at our institution.

Diffusion-Weighted Abnormalities. Regions of restricted diffusion in the immediate vicinity of the resection cav-

Table 1. Patient characteristics for patients demonstrating interim tumor growth versus no growth

	Tumor Growth ($n = 17$)	No Tumor Growth ($n = 15$)
Age (years), median (range)	51 (30–62)	52 (36–73)
Extent of surgical resection (no. patients)		
GTR	7	11
STR	10	4
MIB-1 labeling, median (range) [SD]	23.98 (9.21–82.94[a]) [18.66]	22.86 (7.62–45.63) [10.78]
Postsurgically reduced diffusion (no. patients)	11	10
Days between surgery and pre-RT imaging, median (range)	27 (15–30)	24 (14–29)
New contrast enhancement at pre-RT MRI (no. patients)	17	8
Survival (months), median (95% CI)	15.1 (10.1–20.1)	22.2 (16.7–27.7)
No. patients alive	4/17	5/15

Abbreviations: GTR, gross total resection; STR, subtotal resection; MIB-1, tumor proliferation marker; RT, radiation therapy; CI, confidence interval.

[a]The value of 82.94 appears to be a legitimate outlier; the second closest value in this patient group is 42.92.

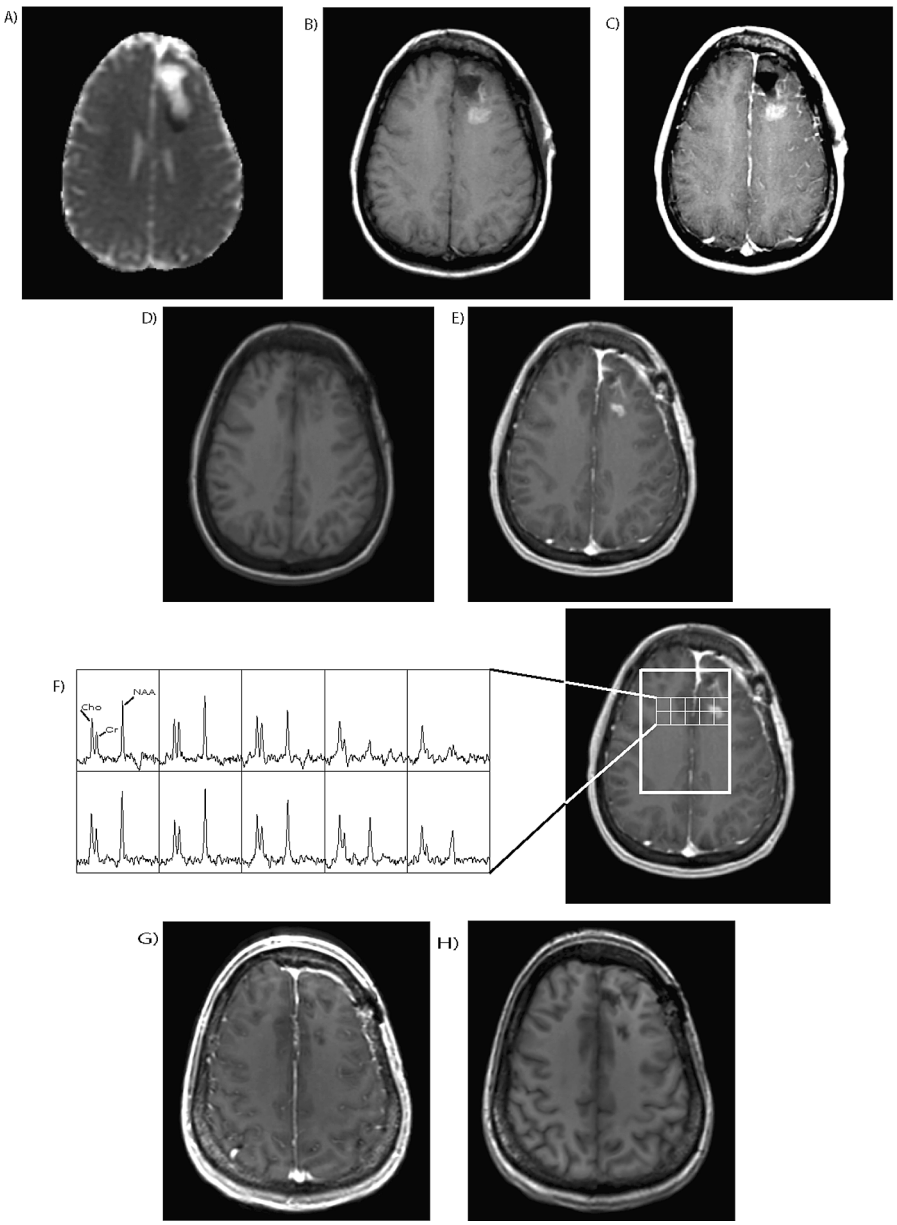

Fig. 1. MR images of a patient after gross surgical resection of a left frontal glioblastoma: at postsurgery (top row), before radiation therapy (RT) (middle two rows), and at follow-up (bottom row). (A) Postoperative diffusion-weighted imaging: apparent diffusion coefficient (ADC) map showing areas of reduced diffusion (dark) along the posterior aspect of the resection cavity. (B and C) Corresponding T1-weighted precontrast (B) and postcontrast (C) spoiled gradient echo (SPGR) images showing some intrinsic T1 shortening on the precontrast scan due to blood products postsurgery, and no contrast enhancement (CE). (D and E) T1-weighted precontrast (D) and postcontrast (E) SPGR images showing a CE nodule in spatial correspondence to the postsurgical regions with reduced diffusion. (F) Spectra from a select region of the CE nodule and contralateral brain tissue showing reduced levels of *N*-acetylaspartate as a sign of compromised neuronal function but no elevation of choline. (G and H) T1-weighted precontrast (G) and postcontrast (H) SPGR images at first follow-up (upon completion of RT), showing complete resolution of the CE nodule and some small focus of encephalomalacia in its place. This patient survived 30.5 months following surgical resection.

ity were seen on postsurgical DW images in 21 patients. These regions exhibited new CE either in part or in their entirety at the pre-RT MRI in 19 patients and were therefore interpreted as a result of postsurgical injury/infarct. Fig. 1 displays a clinical example with DWA at postsurgery imaging and subsequent CE at that same site.

Status Pre-RT

Incidence of New CE. A total of 25 patients demonstrated new or increased CE at pre-RT MRI. The volume ranged from 0.3 to 18.3 cc, with one outlier of 43.8 cc. In eight patients (25%), the new CE was spatially

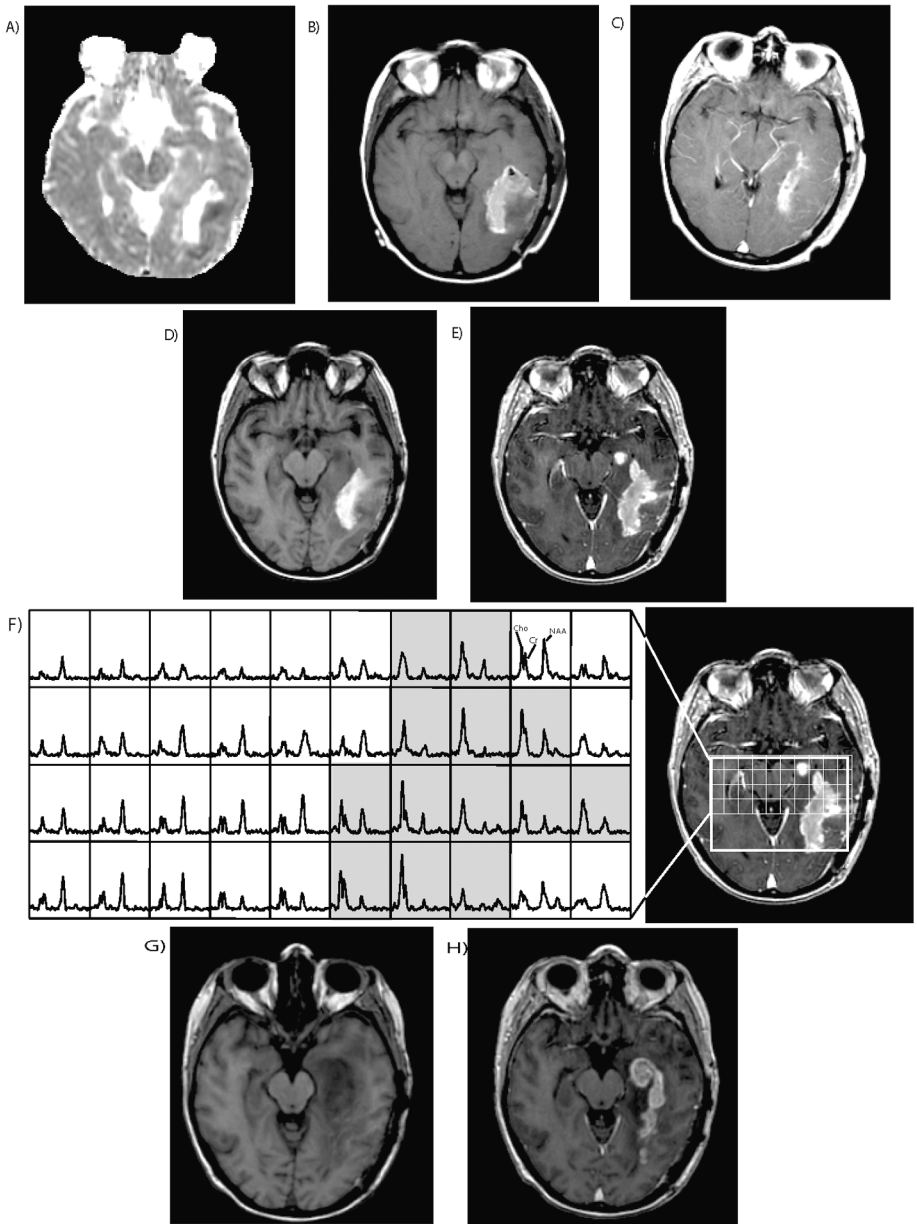

Fig. 2. MR images of a patient after gross total resection of a left temporooccipital glioblastoma: at postsurgery (top row), before radiation therapy (middle two rows), and at follow-up (bottom row). (A) Postoperative diffusion-weighted imaging: apparent diffusion coefficient (ADC) map showing areas of reduced diffusion (dark) along the lateral aspect of the resection cavity. (B and C) Corresponding T1-weighted precontrast (B) and postcontrast (C) spoiled gradient echo (SPGR) images showing some minor intrinsic T1 shortening on the precontrast scan due to blood products postsurgery, and no contrast enhancement (CE). (D and E) T1-weighted precontrast (D) and postcontrast (E) SPGR images showing some CE at the lateral aspect of the resection cavity that was in spatial correspondence to the postsurgical regions with reduced diffusion, and an additional CE nodule anterior to the resection cavity that did not exhibit reduced diffusion at postsurgery ADC, indicating tumor regrowth. (F) Spectra from a select region of the CE nodule, part of the resection cavity, and contralateral brain tissue showing increased levels of choline (and creatine) and reduced levels of *N*-acetylaspartate indicative of tumor metabolism and compromised neuronal function or even neuronal destruction. (G and H) T1-weighted precontrast (G) and postcontrast (H) SPGR images at first follow-up (upon completion of radiation therapy), showing an enlargement and necrotic appearance of the anterior nodule and resolution of the diffusion-weighted abnormality-related CE laterally. This patient survived 11.5 months following surgical resection.

confined and therefore related only to areas of restricted diffusion as assessed postsurgery. In 17 patients (53%), at least some portion of new CE was spatially unrelated to postsurgically reduced diffusion, which was considered indicative of tumor growth in 6 patients (19%) or a combination of tumor growth and postsurgical infarct in 11 patients (34%). Comparison of Figs. 1 and 2 shows a clinical example for purely DWA/infarct-related new CE (Fig. 1) as distinct from new CE presumed to be related to tumor growth (Fig. 2). Volumetric analysis of

Table 2. Pre-radiation therapy MRI parameters (median values) within the region of new contrast enhancement in patients with tumor growth versus no growth

	CE volume (cc)	Cho	CNI	CCrI	ADC
Tumor (n = 17)	5.12	1.28	2.39	1.86	1.46
Postinjury (n = 15)	1.48	0.68	1.32	0.81	1.67
p-Value[a]	0.018	0.01	0.01	0.03	0.08

Abbreviations: CE, contrast enhancement; Cho, choline; CNI, choline-to-*N*-acetylaspartate index; CCrI, choline-to-creatine index; ADC, apparent diffusion coefficient.

[a]Wilcoxon-Mann-Whitney two-sample test.

the regions exhibiting new CE in Fig. 2 revealed that the tumor-growth–related volumes were significantly larger than the DWA-related (no growth) volumes (see Table 2).

Metabolic/Physiologic Imaging Parameters within CE. MRI parameters (see Table 2) obtained within the region of new CE prior to RT demonstrated significantly higher values for Cho, CNI, and CCrI with a trend toward reduced ADC in patients with presumed tumor growth compared to patients with postsurgical infarct, suggesting tumor metabolism and cell proliferation. These data are consistent with our assumption of being able to interpret the cause of new CE as being due to surgical injury (infarct) versus tumor growth. Fig. 3 displays the distribution of parameters found to be significantly different between patients with tumor growth versus no growth.

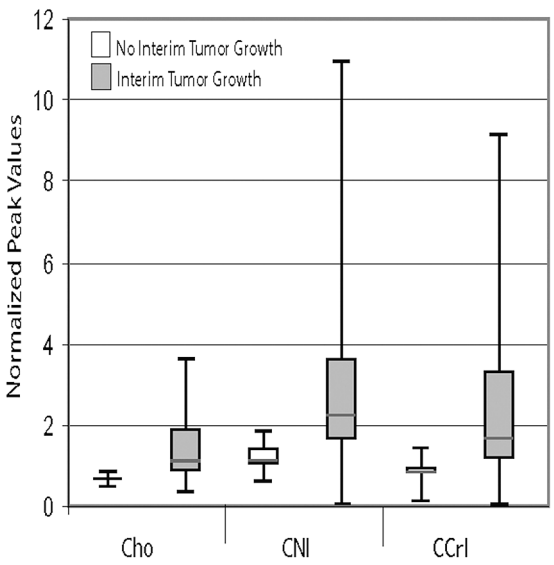

Fig. 3. Box plots of median spectral and diffusion parameters within the region of new contrast enhancement for patients with and without interim tumor growth at pre-radiation therapy MRI; see Table 2 for respective p-values. Displayed data include median (horizontal bar), minimum, 25th and 75th percentiles, and maximum. Abbreviations: Cho, choline; CNI, choline-to-*N*-acetylaspartate index; CCrI, choline-to-creatine index.

Comparison of MIB-1 Labeling Index with or without Interim Tumor Growth. We analyzed the proliferative capacity of each glioblastoma to determine whether this measure predicted a more aggressive tumor as indicated by tumor regrowth prior to RT. A neuropathologist (S.V.) selected appropriate paraffin blocks based on original hematoxylin and eosin stains and, following immunohistochemical staining for Ki-67, determined the MIB-1 labeling index. Twenty-three of 25 glioblastoma paraffin blocks were available at the time of evaluation. MIB-1 labeling indices ranged from 22.9 to 45.6, with one extreme but legitimate value of 82.9. A Wilcoxon-Mann-Whitney test revealed no significant difference for patients with tumor growth versus no growth (p = 0.88; see also Table 1).

Comparison of Survival. Twenty-one (66%) patients were known to have been deceased at the time of analysis. Median follow-up for the remaining 11 patients was 28.1 months (range, 14.3–46.3 months). Overall median survival for all 32 patients included in this study was 18 months (95% confidence interval [CI], 14–22 months). There was no statistical relationship between MIB-1 and survival (Wilcoxon test, p = 0.47) in our patient population.

Tumor growth versus no growth: Kaplan-Meier survival analyses were performed and are displayed in Fig. 4. The median survival was 14.6 months (95% CI, 9.1–20.1 months) in patients with interim tumor growth compared to 24 months (95% CI, 18.9–29.1 months) in patients who did not demonstrate tumor growth. The graphs extend to 36 months, because only four patients survived past this time point (39.3, 43.6, 46.2, and 46.3 months). The log-rank test was not statistically significant (p = 0.11). The Wilcoxon test, which is more sensitive to differences in early time points between groups, was statistically significant (p = 0.022).

Extent of surgery: We found no difference in survival relative to the extent of surgery as assessed by standard radiographic criteria. Median survival for patients with GTR was 18.7 (95% CI, 13.3–24.1) months and for patients with STR was 16.8 (95% CI, 10.9–22.7) months. Fig. 4 displays survival curves for patients after GTR versus STR. The associated log-rank p-value is 0.28.

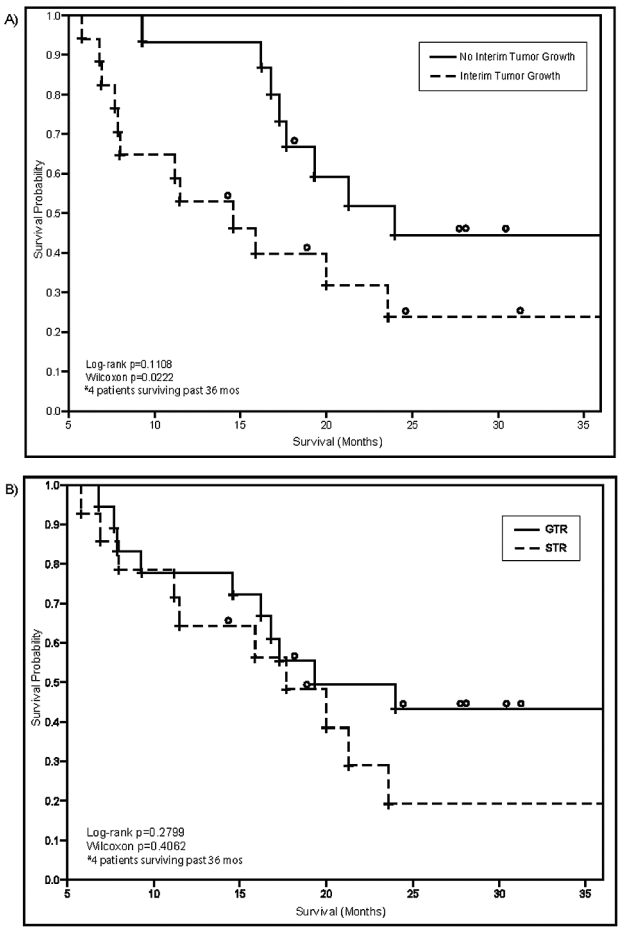

Fig. 4. Kaplan-Meier survival curves for patients with and without interim tumor growth between surgery and pre-RT imaging (A) and patients with gross total versus subtotal resection (B). The graphs extend to 36 months because only four patients survived past this time point.

Tumor growth versus no growth relative to extent of surgery: Based on estimated survival curves, the suggested advantage in near-term survival in patients without interim tumor growth does not appear to be associated with the degree of surgical resection.

Status Presurgery

Quantitative MR Measures. Metabolic and physiologic MRI data acquired prior to surgery indicated that higher perfusion and Cr values within the nonenhancing portion of the tumor predicted subsequent tumor growth in respective patients. However, within the CE portion of the tumor, no imaging parameters appeared related to or predictive of tumor growth versus no growth. Similarly, none of the standard volumetric MR measures differed between patient groups. Table 3 and Fig. 5 summarize our results.

Discussion

New regions of CE were seen in 78% (25 of 32) of patients with newly diagnosed glioblastoma at about 4 weeks following surgical resection. These were spatially correlated with regions of postsurgically restricted diffusion and could therefore be interpreted as a delayed sign of infarct in 32% (8 of 25) of the patients. In most cases, this resolved during subsequent follow-ups and turned into foci of encephalomalacia within a time frame similar to that presented in detail in a recent publication from our institution[14] and as summarized in the introduction. Without the correlation to postsurgical DWI, the imaging results from these patients could easily have been misinterpreted as tumor growth.

In 68% (17 of 25) of the patients who developed new CE during the time interval between surgery and the beginning of RT, there was no corresponding DWA in the postsurgery examination. This new CE was interpreted as tumor growth due to the quantitative metabolic/physiologic characteristics of residual microscopic disease with aggressive behavior and higher proliferative capacity. The presence of new CE was associated with significantly shorter survival according to the Wilcoxon test but did not reach significance based on the log-rank test. The former emphasizes differences in survival during early time points, while the latter is associated with longer term behavior. The results of the analysis may also be confounded by the fact that patients with longer survival may have undergone multiple subsequent therapies. Further studies are required to determine whether the results hold up in a larger population of patients.

The MIB-1 labeling index that was determined from tissue removed during surgical resection was not predictive of tumor growth or survival in our study population. In contrast, imaging parameters within the nonenhancing lesion component of the tumor that were assessed 1 day prior to surgery were predictive of the likelihood of tumor growth. These differences may be explained by the MIB-1 index having been determined from the resected tissue, which is for the most part CE "gross disease," while the nonenhancing lesion is more likely to remain unresected. We observed from our data that when these regions exhibited tumor-suggestive physiologic and metabolic characteristics indicative of angiogenesis (elevated CBV and PH) and increased bioenergetics (increased Cr) relative to contralateral brain tissue, the occurrence of new CE corresponding to tumor growth was more likely between surgery and the start of adjuvant therapy. Note that the term "tumor growth" may be misleading in this context because the observed changes are occurring in regions of T2 hyperintensity that were previously nonenhancing but do contain measurable tumor infiltration according to physiologic and metabolic MRI parameters. These findings suggest that advanced MRI modalities may be useful in presurgical planning to help delineate a maximal safe resection that considers all regions suggestive of tumor.

While the clinical benefit of more extensive surgical resection in glioblastoma remains controversial, Lacroix et al.[7] demonstrated in a large retrospective study a sur-

Table 3. Presurgery MRI parameters (median values) with respect to prediction of tumor growth during the interval between surgery and beginning of radiation therapy

	Volume of CE (cc)	Volume of T2 Hyperintensity (cc)	CBV within NEL	PH within NEL	Cr within NEL
Tumor	14.97	43.29	1.37	1.24	1.03
Postinjury	18.18	52.75	0.80	0.81	0.60
p-Value[a]	0.94	0.35	0.006	0.009	0.03

Abbreviations: CE, contrast enhancement; CBV, cerebral blood volume; NEL, nonenhancing lesion; PH, peak height; Cr, creatine.

[a]Wilcoxon-Mann-Whitney two-sample test.

vival benefit for patients following GTR and chemotherapy compared to STR for glioblastoma. This was particularly evidenced in patients with favorable prognostic variables. Although survival did not differ in our patients following GTR or STR, the median survival of our population was 5.7 months longer for patients with GTR and 8 months longer for the patients with STR relative to Lacroix's data. In addition, the degree of tissue removal following STR was estimated with a median of 90% for our patient group and was thereby vastly more extensive than that reported in Lacroix's patient population. This, together with growing evidence of increased effectiveness of agents used in the adjuvant and post-progression setting, may explain the indifference in survival relative to the extent of resection in this study.[1,24]

On a related note, another recent study from our group examined the predictive value of pre-RT MR parameters in relation to survival in patients with newly diagnosed, resected glioblastoma.[25] Anatomic, physiologic, and metabolic measures of residual tumor volume correlated strongly with survival. In particular, CNI > 2, CBV > 3, and ADC < 1.5 times those in normal white matter were each found to be strongly associated with decreased survival. This indicates that patients with larger residual tumor burden tended to have a higher risk for poor survival and further supports the concept

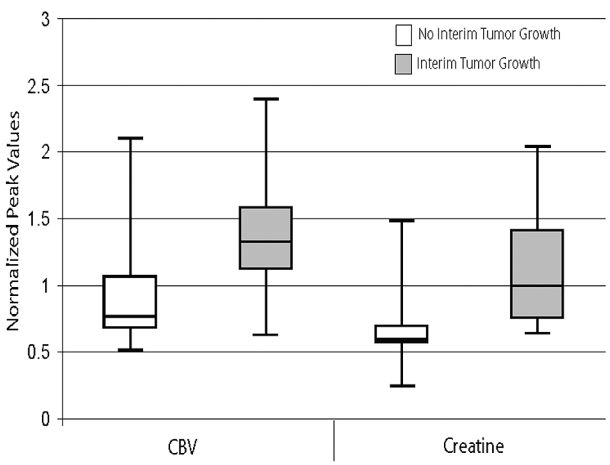

Fig. 5. Box plots of median perfusion and spectral parameters within the presurgical nonenhancing lesion component of the tumor for patients with and without interim tumor growth; see Table 3 for corresponding *p*-values. Displayed data include median (horizontal bar), minimum, 25th and 75th percentile, and maximum. Abbreviation: CBV, cerebral blood volume.

of achieving a maximal safe tumor resection in patients with glioblastoma. While there are obvious anatomic, functional, and other limitations to achieving a maximal safe resection, the inclusion of advanced imaging modalities has the potential to define regions that exhibit tumor characteristics beyond the region of CE that could be considered for resection.

Within the overall glioblastoma patient population, tumor growth occurred in 53% of patients and varied greatly from patient to patient as assessed at 4 weeks (±2 weeks) following surgical resection of the tumor. On a case-by-case basis, the degree of tumor growth did not correlate with the time interval between surgery and pre-RT imaging (see also Table 1). This demonstrates the differing dynamics and underlying biologic properties of individual lesions. While we cannot exclude the possibility that CE in adjacent noninfarcted tissues reflect vascular changes, we showed that regions of CE deemed to be related to tumor growth exhibited metabolic and physiologic characteristics of tumor-suggestive metabolism and proliferation and increased cell density in comparison to the characteristics of the CE regions that corresponded to DWAs. The data presented support the value of advanced MRI modalities in distinguishing the cause of CE prior to adjuvant therapy and should be incorporated in the baseline imaging for patients entering clinical trials that seek to assess the effectiveness of investigational agents.

In addition to the implications of our findings for surgical planning and the baseline assessment of patients participating in clinical trials, we believe they raise questions with regard to the timing of initiation of adjuvant therapy and offer the opportunity for customized target definition for RT planning. The fact that tumor growth occurs in more than half of the glioblastoma patients during the 4-week period between surgery and initiation of RT suggests that it may be worthwhile to consider shortening this time interval. Decades ago RT was carried out with cobalt or orthovoltage equipment that had low-depth dose characteristics and caused wound breakdown. During the early days of megavoltage (MV) irradiation, opposing lateral radiation fields were customarily employed to deliver whole-brain and later partial-brain RT, causing acute toxicity to the skin and ear. With the advent of MV irradiation, dose has been escalated gradually while decreasing such toxicity.[26] Modern RT is customarily carried out as three-dimensional conformal RT, preferably with a 6-MV photon linear accelerator that employs four or more noncoplanar radiation fields to conform the prescribed dose to the tumor, while sparing surrounding tissue. In practice,

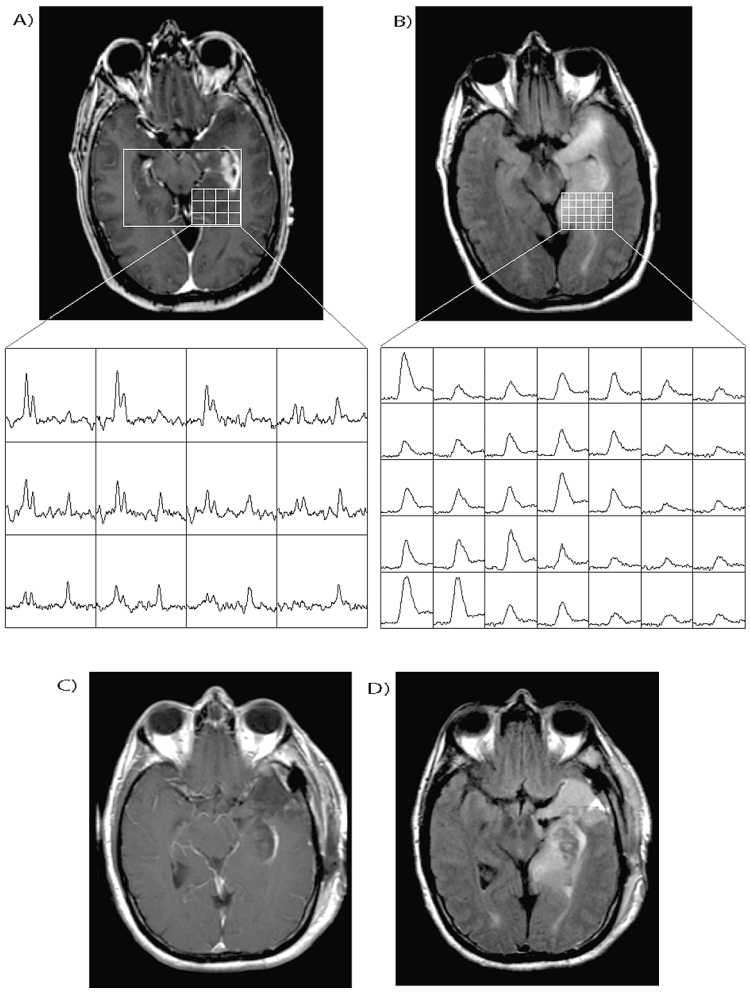

Fig. 6. Patient with left temporal glioblastoma prior to (top) and immediately after (bottom) surgery. (A) T1-weighted postcontrast spoiled gradient echo (SPGR) image showing the contrast-enhancing lesion with central necrosis. (B) Fluid-attenuated inversion recovery (FLAIR) image showing extensive T2 hyperintensity. Superimposed on A and B are regions of data acquisition and magnified, respective spectra and perfusion curves from the posterior, nonenhancing aspect of the tumor showing tumor suggestive metabolism with elevated choline and creatine and diminished *N*-acetylaspartate, as well as tumor vasculature suggestive perfusion curves with high amplitude and lack of recovery back to baseline. (C and D) T1-weighted postcontrast SPGR (C) and FLAIR showing status postsubtotal resection (D): resection cavity following temporolobectomy, some residual contrast enhancement lining the lateral aspect of the resection cavity (status after subtotal resection) and remaining FLAIR hyperintensity. Note that the posterior, nonenhancing portion of the tumor with tumor suggestive metabolism and neovasculature remained.

RT can start as early as when postsurgical tissue swelling resolves and the patient is considered to have adequately recovered. For these reasons, our recommendation would be to consider starting RT and concurrent chemotherapy with temozolomide 2 weeks following surgery, if the patient's general status permits. Whether this would positively affect patient outcome is beyond the scope of this study and should be tested in a clinical trial.

Another potential value of acquiring MR images prior to preadjuvant therapy is in refining the target definition for RT. It is widely accepted that MRI provides better soft tissue contrast than does CT for treatment planning. Some institutional policies call for the correlation of presurgical MRI with the treatment planning CT to assist in prescribing the target for RT. Most institutions have adapted the policy to define target volumes based on postsurgical MRI with the goal of covering the primary/residual lesion enlarged by a few centimeters. Current Radiation Therapy Oncology Group clinical trials call for prescribing a dose of 46 Gy to a region that includes a 2-cm margin around the hyperintensity on T2-weighted MR images, and prescribing an additional dose of 14 Gy (cone down) to a second volume defined by the CE on the T1-weighted postcontrast MR images plus a 2.5-cm margin.

Pennington et al.[27] evaluated tumor growth relative to postoperative MRI in 10 patients with glioblastoma during the period prior to RT. They showed that tumor growth (increase in CE) occurred within a 2-cm margin of the residual postoperative tumor. While we observed that CE occurred in close proximity to the residual tumor/resection cavity, we did not attempt to

compare the spatial extent of postsurgical and pre-RT CE volumes because of the uncertainty associated with aligning these two imaging scans, which often exhibit significant tissue shifts following extensive tumor resection. We have previously analyzed the value of combined MRI and MRSI for customized target definition prior to RT and found that the incorporation of areas of metabolic abnormality into treatment planning would produce target volumes with different sizes and shapes for both primary and boost volumes.[28] This would offer the opportunity to significantly reduce treatment margins with a reduction in radiation exposure and toxicity for regions of normal brain.

In summary, we believe that our findings have implications for surgical and RT planning as well as the assessment of therapeutic response in the context of clinical trials. Our study also raises questions regarding the current time interval between surgery and initiation of adjuvant therapy.

Acknowledgments

This work was supported in part by National Cancer Institute grants P50 CA97257 and R01 CA59880.

References

1. Stupp R, Mason WP, van den Bent MJ, et al. Radiotherapy plus concomitant and adjuvant temozolomide for glioblastoma. *N Engl J Med*. 2005;352:987–996.
2. Surawicz TS, Davis F, Freels S, et al. Brain tumor survival: results from the National Cancer Data Base. *J Neurooncol*. 1998;40:151–160.
3. Wrensch M, Minn Y, Chew T, et al. Epidemiology of primary brain tumors: current concepts and review of the literature. *Neuro-Oncology*. 2002;4:278–299.
4. Scott JN, Rewcastle NB, Brasher PM, et al. Which glioblastoma multiforme patient will become a long-term survivor? A population-based study. *Ann Neurol*. 1999;46:183–188.
5. Burger PC, Green SB. Patient age, histologic features, and length of survival in patients with glioblastoma multiforme. *Cancer*. 1987;59:1617–1625.
6. Albert FK, Forsting M, Sartor K, et al. Early postoperative magnetic resonance imaging after resection of malignant glioma: objective evaluation of residual tumor and its influence on regrowth and prognosis. *Neurosurgery*. 1994;34:45–61.
7. Lacroix M, Abi-Said D, Fourney DR, et al. A multivariate analysis of 416 patients with glioblastoma multiforme: prognosis, extent of resection, and survival. *J Neurosurg*. 2001;95:190–198.
8. Montine TJ, Vandersteenhoven JJ, Aguzzi A, et al. Prognostic significance of Ki-67 proliferation index in supratentorial fibrillary astrocytic neoplasms. *Neurosurgery*. 1994;34:674–679.
9. Reavey-Cantwell JF, Haroun RI, Zahurak M, et al. The prognostic value of tumor markers in patients with glioblastoma multiforme: analysis of 32 patients and review of the literature. *J Neurooncol*. 2001;55:195–204.
10. Hegi ME, Diserens AC, Gorlia T, et al. MGMT gene silencing and benefit from temozolomide in glioblastoma. *N Engl J Med*. 2005;352:997–1003.
11. Henegar MM, Moran CJ, Silbergeld DL. Early postoperative magnetic resonance imaging following nonneoplastic cortical resection. *J Neurosurg*. 1996;84:174–179.
12. Cairncross JG, Pexman JH, Rathbone MP, et al. Postoperative contrast enhancement in patients with brain tumor. *Ann Neurol*. 1985;17:570–572.
13. Forsting M, Albert FK, Kunze S, et al. Extirpation of glioblastomas: MR and CT follow-up of residual tumor and regrowth patterns. *AJNR Am J Neuroradiol*. 1993;14:77–87.
14. Smith JS, Cha S, Mayo MC, et al. Serial diffusion-weighted magnetic resonance imaging in cases of glioma: distinguishing tumor recurrence from postresection injury. *J Neurosurg*. 2005;103:428–438.
15. Ulmer S, Braga TA, Barker FG 2nd, et al. Clinical and radiographic features of peritumoral infarction following resection of glioblastoma. *Neurology*. 2006;67:1668–1670.
16. Daumas-Duport C, Beuvon F, Varlet P, et al. [Gliomas: WHO and Sainte-Anne Hospital classifications] [in French]. *Ann Pathol*. 2000;20:413–428.
17. Nelson SJ, Nalbandian AB, Proctor E, et al. Registration of images from sequential MR studies of the brain. *J Magn Reson Imaging*. 1994;4:877–883.
18. Lupo JM, Cha S, Chang SM, et al. Dynamic susceptibility-weighted perfusion imaging of high-grade gliomas: characterization of spatial heterogeneity. *AJNR Am J Neuroradiol*. 2005;26:1446–1454.
19. Tran TK, Vigneron DB, Sailasuta N, et al. Very selective suppression pulses for clinical MRSI studies of brain and prostate cancer. *Magn Reson Med*. 2000;43:23–33.
20. Star-Lack J, Spielman D, Adalsteinsson E, et al. In vivo lactate editing with simultaneous detection of choline, creatine, NAA, and lipid singlets at 1.5 T using PRESS excitation with applications to the study of brain and head and neck tumors. *J Magn Reson*. 1998;133:243–254.
21. Nelson SJ, Day MR, Buffone PJ, et al. Alignment of volume MR images and high resolution [18F]fluorodeoxyglucose PET images for the evaluation of patients with brain tumors. *J Comput Assist Tomogr*. 1997;21:183–191.
22. Nelson SJ. Analysis of volume MRI and MR spectroscopic imaging data for the evaluation of patients with brain tumors. *Magn Reson Med*. 2001;46:228–239.
23. McKnight TR, Noworolski SM, Vigneron DB, et al. An automated technique for the quantitative assessment of three-dimensional-MRSI data from patients with glioma. *J Magn Reson Imaging*. 2001;13:167–177.
24. Kreisl TN, Kim L, Moore K, et al. Phase II trial of single-agent bevacizumab followed by bevacizumab plus irinotecan at tumor progression in recurrent glioblastoma. *J Clin Oncol*. 2009;27(5):740–5.
25. Saraswathy S, Crawford F, Lamborn K, et al. Evaluation of pretreatment MR markers that predict survival in patients with newly diagnosed GBM.
26. Walker MD, Strike TA, Sheline GE. An analysis of dose-effect relationship in the radiotherapy of malignant gliomas. *Int J Radiat Oncol Biol Phys*. 1979;5:1725–1731.
27. Pennington C, Kilbride L, Grant R, et al. A pilot study of brain tumour growth between radiotherapy planning and delivery. *Clin Oncol (R Coll Radiol)*. 2006;18:104–108.
28. Pirzkall A, Li X, Oh J, et al. 3D MRSI for resected high-grade gliomas before RT: tumor extent according to metabolic activity in relation to MRI. *Int J Radiat Oncol Biol Phys*. 2004;59:126–137.